Supplementary Information (SI) for New Journal of Chemistry.

Supplementary information for

A DFT study on the surface reaction mechanisms on 4H-SiC surfaces with gaseous species from MTS-H_2 gas-phase system

Botao Song, Bing Gao*, Sheng Liu*, Yan Zhao, and Fang Dong

The Institute of Technological Sciences, Wuhan University, Wuhan 430072, China.

* Corresponding authors.

E-mail address: gaobing@whu.edu.cn (Bing Gao).

E-mail address: shengliu@whu.edu.cn (Sheng Liu).

Table S1 Point groups and molecular mass of gas phase species*.

gas phase species	C_2H_6	C_2H_5	CH_4	CH_3	CH_3Cl	CH_2
point group	D_{3d}	C_s	T_d	D_{3h}	C_{3v}	C_{2v}
molecular mass (amu)	30.047	29.039	16.031	15.023	49.992	14.016
gas phase species	C_2H_4	$SiCl_4$	$SiCl_3$	$SiHCl_3$	$SiCl_2$	HCl
point group	D_{2h}	T_d	C_{3v}	C_{3v}	C_{2v}	$C_{\infty v}$
molecular mass (amu)	28.031	167.852	132.883	133.891	97.915	35.977
gas phase species	H	Cl	CH_3SiHCl_2			
point group	C_1	C_1	C_s			
molecular mass (amu)	1.008	34.969	113.946			

* The point groups of gas phase species employed in the calculation of rotational partition function and the molecular mass employed in the calculations are listed in this table.

Section S1

For the reactions without a distinct transition state configuration through scanning the molecular potential energy surface (PES) of the electronic energy to the saddle point, the canonical variational transition state theory (CVTST) with Baik method[1] was employed to identify the generalized transition state. The configuration of the cluster with adsorbed surface species at optimized equilibrium state is defined as the initial state. The state wherein the gaseous particle and the cluster of the adsorbent with a dangling bond are situated at an infinite separation is designated as the final state. The initial state is indicative of the product of an adsorption reaction, whereas the final state is representative of the reactants. For reactions without a distinct transition state, there are various flexible scanning steps that have been systematically conducted for constrained configuration optimizations along each adsorption path.

Consider the adsorption process of $SiCl_3$ to the surface site O_{Si}(ads) as an exemplar for explication. Exploring the stepwise bond-breaking process as illustrated in Figure S1(a). The calculated values of electronic energies increase with stepwise elongation from the initial state. The value of electronic energy at the final state is taken as the sum of the energy of gaseous species and the energy of the adsorbent. Take the calculated energy of the initial state, the calculated energy of the final state, and the calculated energies during the stepwise elongation process as sampling data points. The differential values, ΔE(SCF), are ascertained by computing the deviation of the calculated energies from the calculated energy of the initial state. The calculated values of ΔE(SCF) are denoted by red squares, as illustrated in Figure S1(b). Then the calculated energies have been fitted to the Morse function[2], represented by a black solid curve in Figure S1(b). It should be noted that, the employment of Baik's method necessitates the assumption that no local maxima exist on the fitted curve between the initial state and the final state[1], which implies that the energy increases monotonically during the desorption process. However, in this study, for the calculated bond-breaking reactions, if the computed energy along the bond-breaking path does not increase monotonically, a Gaussian term is added to Morse function to correct the fitting curve.

The term related to entropy, $-TS$, make a relatively large contribution to the correction of Gibbs free energy. As the separation between desorption species and the adsorbent keeps extending, as demonstrated in Baik's work[2], the approach to translational entropy becomes progressively inadequate, leading to the calculated values of entropy become increasingly incorrect. To estimate the terms related to thermochemistry in a more appropriate way, the computed data of a few configurations in the initial stage of scanning and the final state are utilized as sampling points. Take thermal correction to Gibbs free energies (G_corr) at 1200 K as an example, the differential values of G_corr, ΔG_corr, are ascertained by computing the deviation of the calculated values of the first few scanning configurations from the calculated value of the initial state. The G_corr at the final state is taken as the sum of the G_corr of gaseous species and the G_corr of the adsorbent. The calculated values of ΔG_corr are denoted by red squares, as illustrated in Figure S1(c). Then the calculated values of ΔG_corr have been fitted to a sigmoidal function, represented by a black solid curve in Figure S1(c).

The fitted curve of ΔE(SCF) and the fitted curve of ΔG_corr at 1200 K can be combined to obtain the fitted curve of ΔG at 1200 K as illustrated in Figure S1(d), the free energy barrier for adsorption at 1200 K is about 6.9 kcal/mol, while the free energy barrier for desorption is about 45.1 kcal/mol. The curve for ΔZPE as shown in Figure S1(e), was fitted in the same way which was employed to fitting the curve of ΔG_corr. Then we can obtain the fitted curve of ΔE(SCF)+ΔZPE as illustrated in Figure S1(f), in the same way we acquire the ΔG curve. Therefore, the energy of activation at 0 K for the adsorption process is zero, while that for the desorption process is about 72.9 kcal/mol.

In this study, we anticipated that the estimated value of the partition function at the generalized transition state is more likely closer to the value of the partition function of the initial state. Therefore, for reactions without a distinct transition state, employe the partition function of the sixth configuration alone the scanning path from the initial state as the partition function of the generalized transition state, literally the term q_{TS} in equation (4) in the manuscript. It can be anticipated that this assumption might introduce errors to a certain degree, but within an acceptable margin.

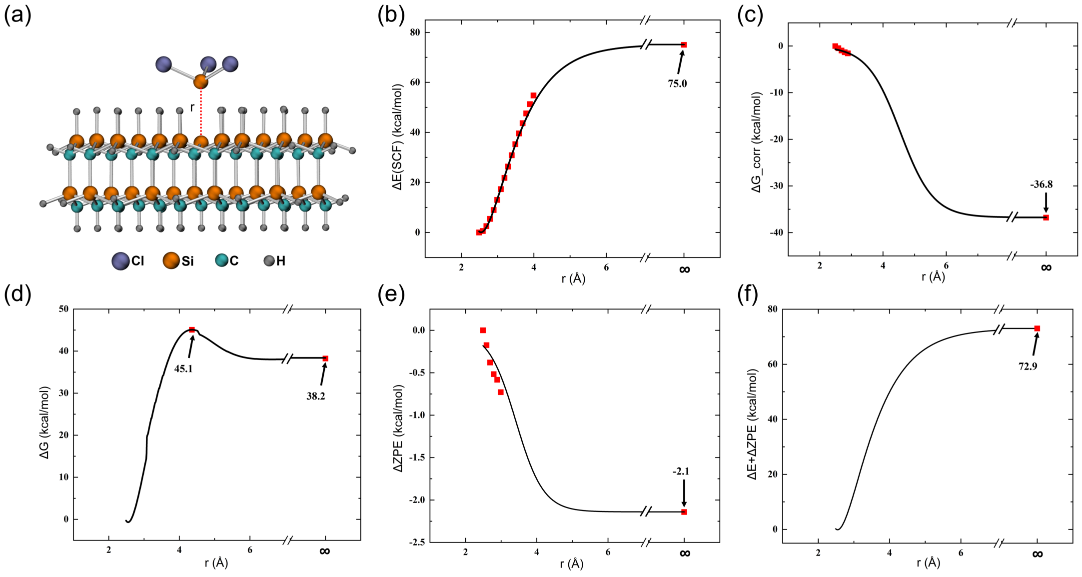

Figure S1 (a) Schematic illustration of the adsorption process of $SiCl_3$ on (0001) face, the computed (red scatter points) and fitted (curve) profiles of (b) electronic energies (E(SCF)), (c) the thermal correction to Gibbs free energies (G_corr) at 1200 K and (e) zero-point energies (ZPE) along the adsorption path; the profiles of (d) Gibbs free energies (G) at 1200 K and (f) internal energy (E(SCF)+ZPE) along the adsorption path.

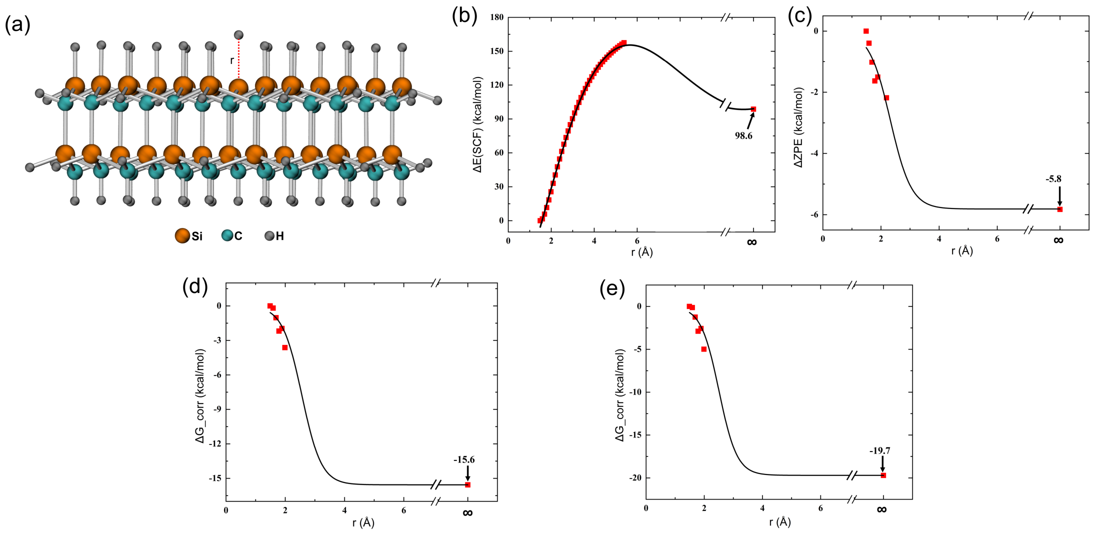

Figure S2. (a) Schematic illustration of the adsorption process of H on (0001) face, the computed (red scatter points) and fitted (curve) profiles of (b) electronic energies, (c) zero-point energies (ZPE), and the thermal correction to Gibbs free energies (G_corr) along the adsorption path at (d) 1200 K and (e) 1800 K.

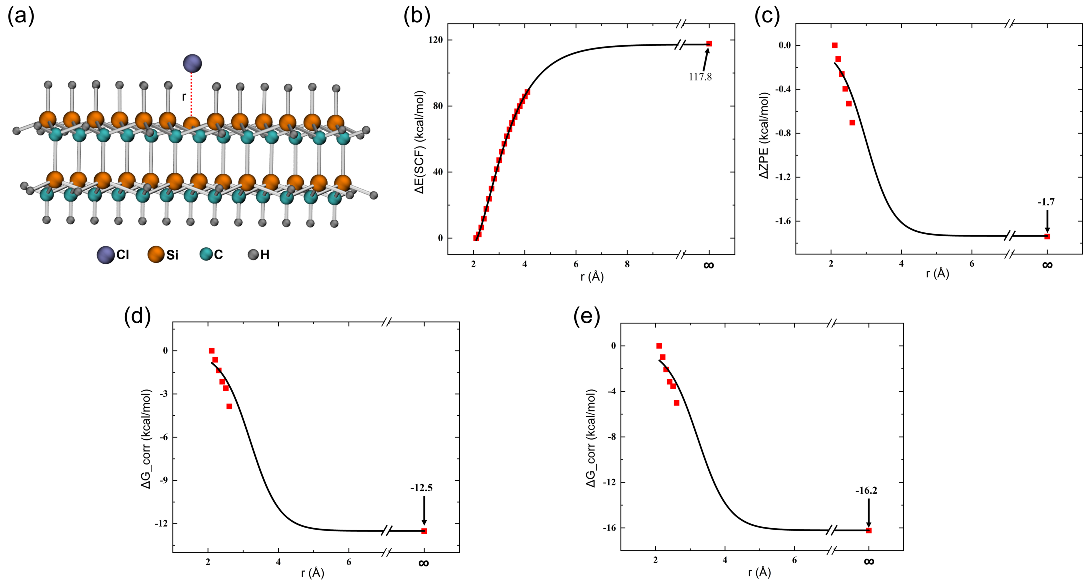

Figure S3 (a) Schematic illustration of the adsorption process of Cl on (0001) face, the computed (red scatter points) and fitted (curve) profiles of (b) electronic energies, (c) zero-point energies (ZPE), and the thermal correction to Gibbs free energies (G_corr) along the adsorption path at (d) 1200 K and (e) 1800 K.

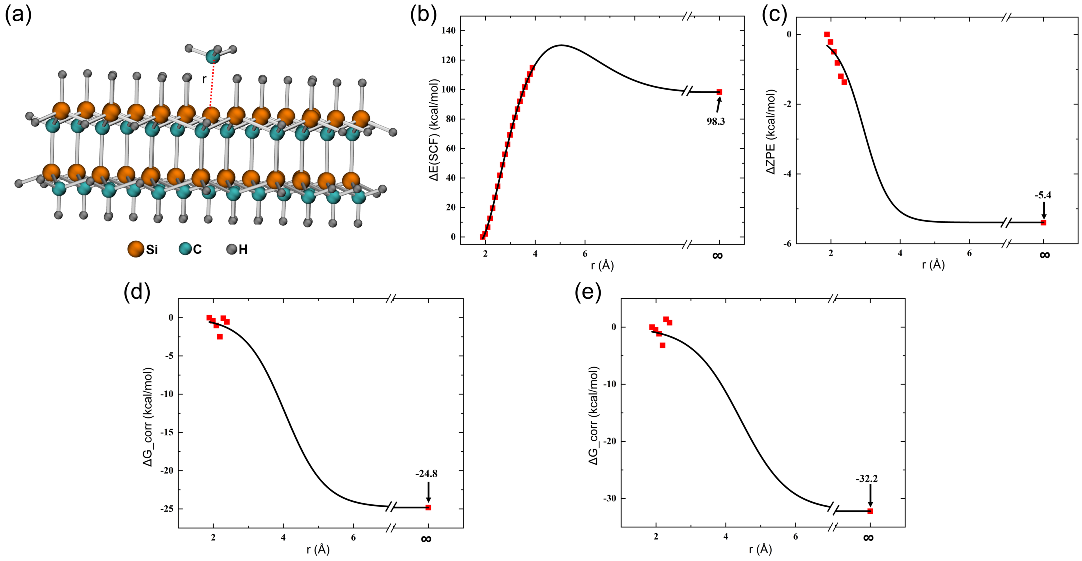

Figure S4. (a) Schematic illustration of the adsorption process of CH_3 on (0001) face, the computed (red scatter points) and fitted (curve) profiles of (b) electronic energies, (c) zero-point energies (ZPE), and the thermal correction to Gibbs free energies (G_corr) along the adsorption path at (d) 1200 K and (e) 1800 K.

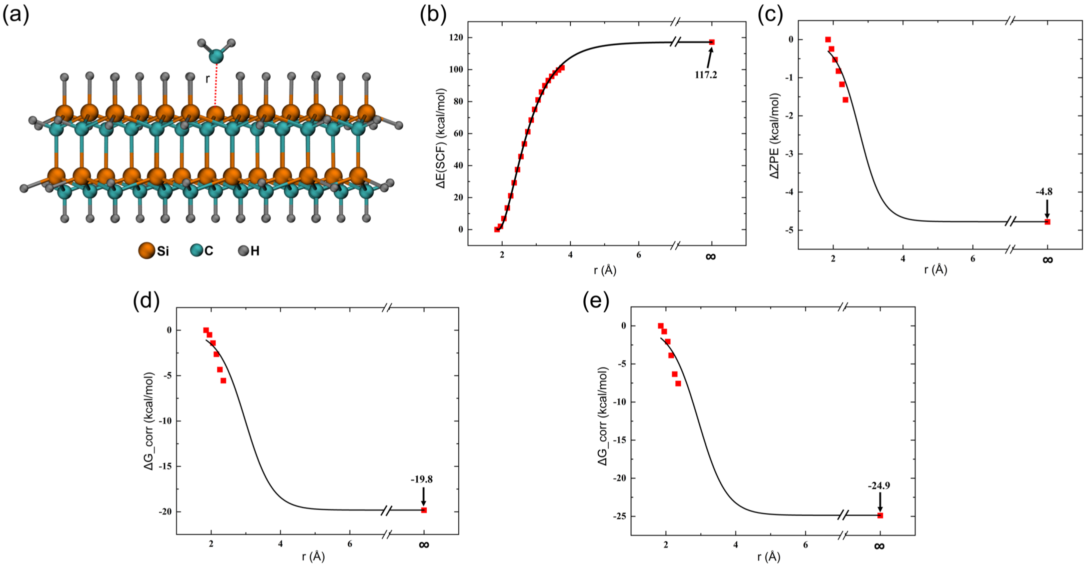

Figure S5. (a) Schematic illustration of the adsorption process of CH_2 on (0001) face, the computed (red scatter points) and fitted (curve) profiles of (b) electronic energies, (c) zero-point energies (ZPE), and the thermal correction to Gibbs free energies (G_corr) along the adsorption path at (d) 1200 K and (e) 1800 K.

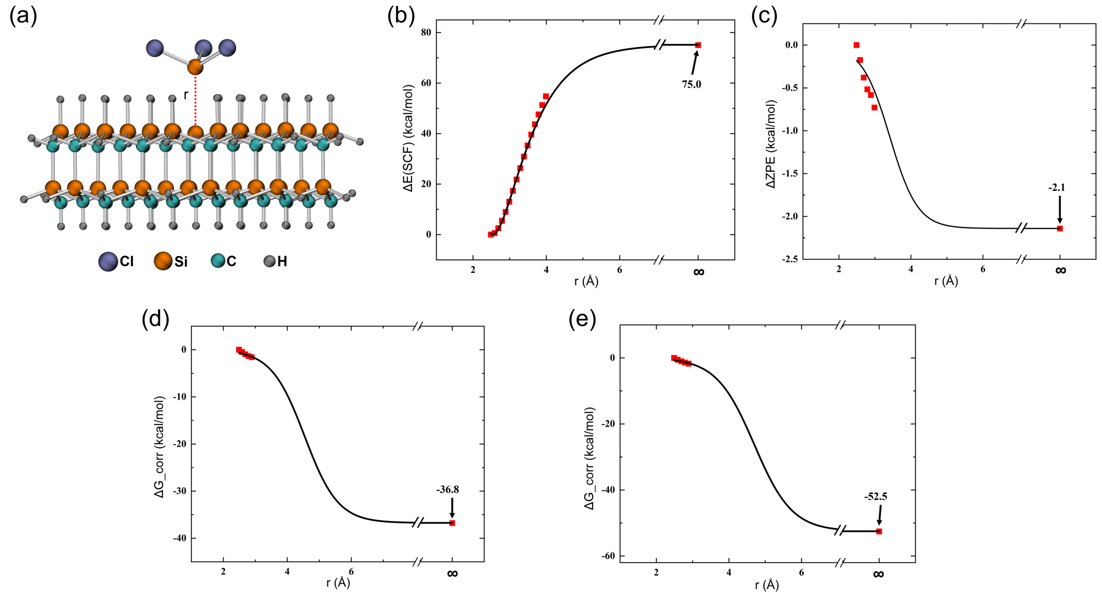

Figure S6. (a) Schematic illustration of the adsorption process of $SiCl_3$ on (0001) face, the computed (red scatter points) and fitted (curve) profiles of (b) electronic energies, (c) zero-point energies (ZPE), and the thermal correction to Gibbs free energies (G_corr) along the adsorption path at (d) 1200 K and (e) 1800 K.

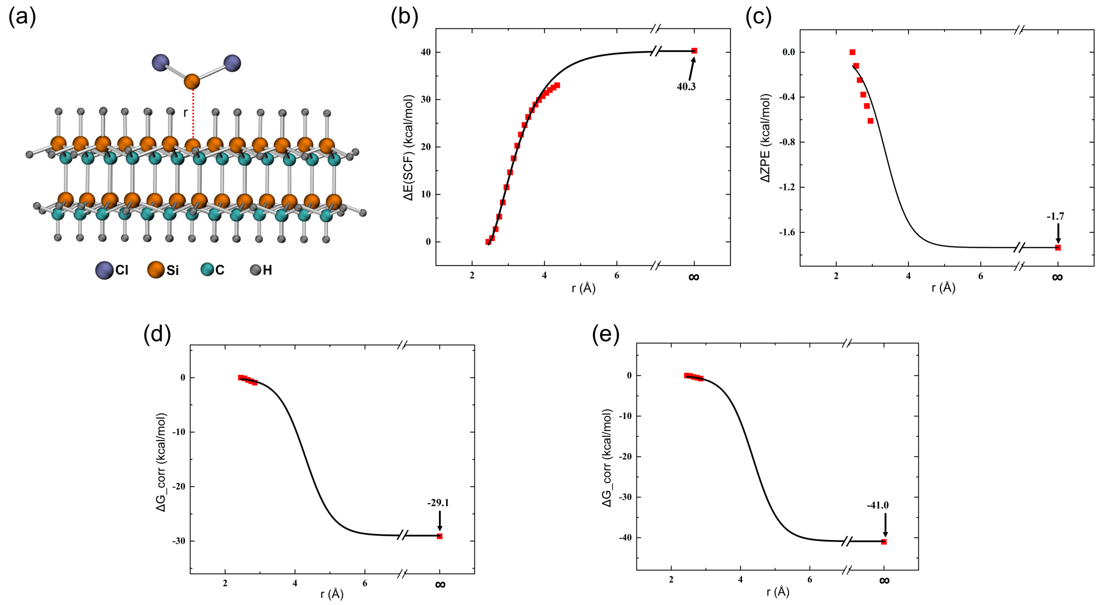

Figure S7. (a) Schematic illustration of the adsorption process of $SiCl_2$ on (0001) face, the computed (red scatter points) and fitted (curve) profiles of (b) electronic energies, (c) zero-point energies (ZPE), and the thermal correction to Gibbs free energies (G_corr) along the adsorption path at (d) 1200 K and (e) 1800 K.

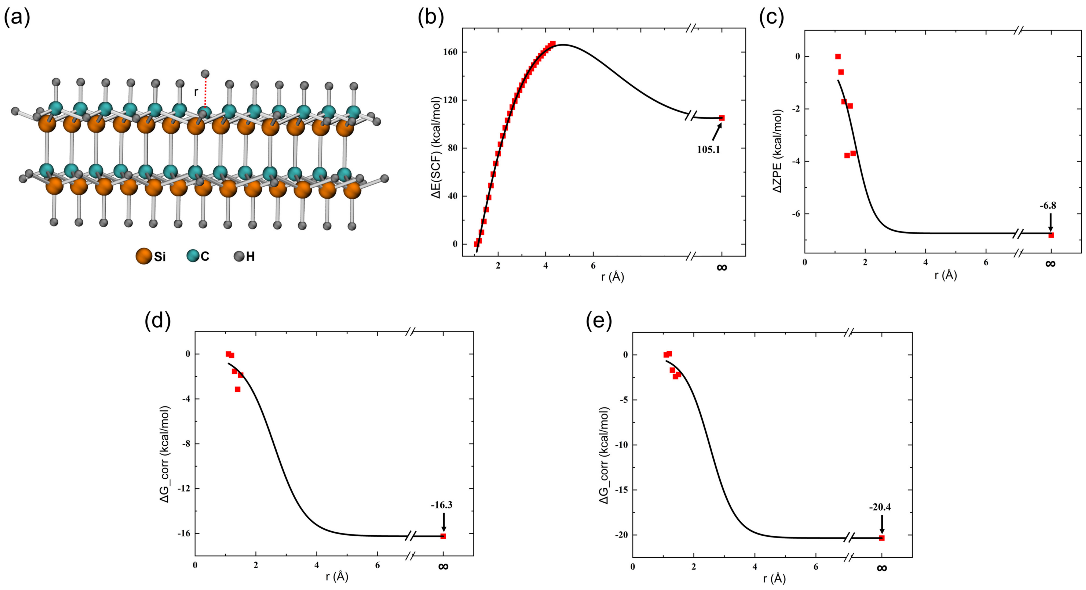

Figure S8. (a) Schematic illustration of the adsorption process of H on $(000\bar{1})$ face, the computed (red scatter points) and fitted (curve) profiles of (b) electronic energies, (c) zero-point energies (ZPE), and the thermal correction to Gibbs free energies (G_corr) along the adsorption path at (d) 1200 K and (e) 1800 K.

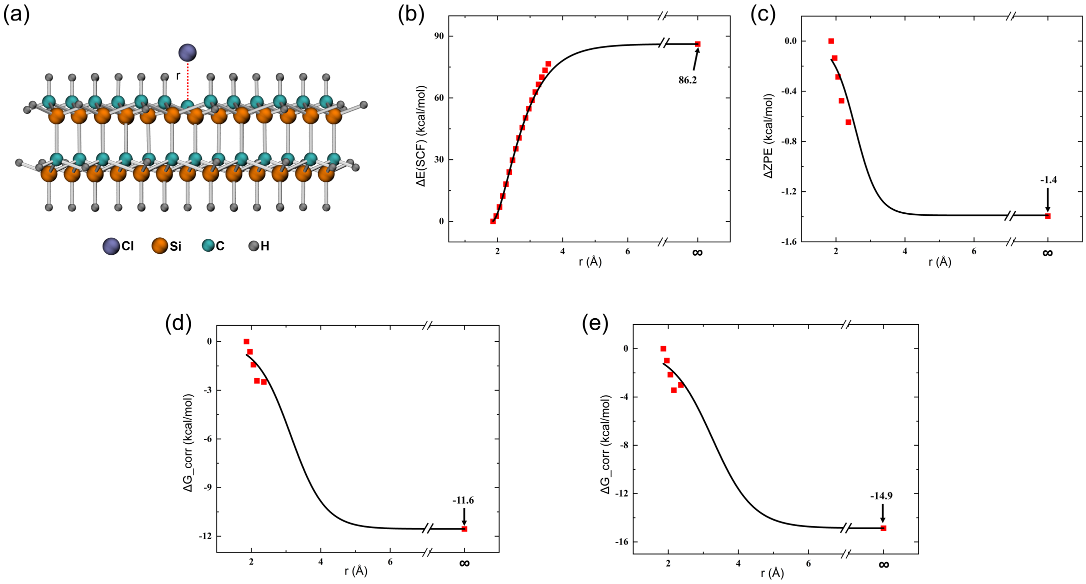

Figure S9. (a) Schematic illustration of the adsorption process of Cl on $(000\bar{1})$ face, the computed (red scatter points) and fitted (curve) profiles of (b) electronic energies, (c) zero-point energies (ZPE), and the thermal correction to Gibbs free energies (G_corr) along the adsorption path at (d) 1200 K and (e) 1800 K.

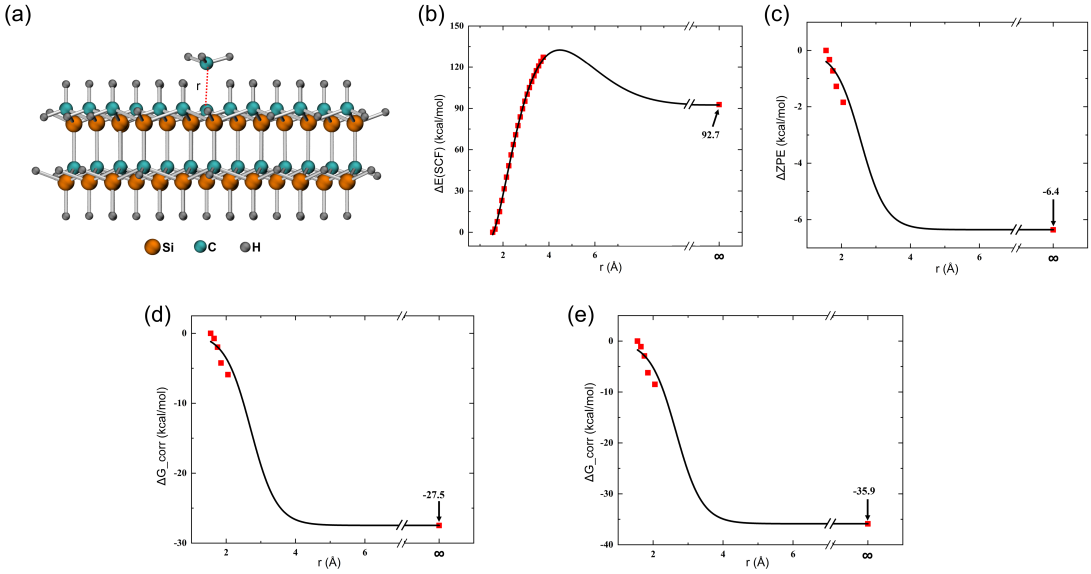

Figure S10. (a) Schematic illustration of the adsorption process of CH_3 on $(000\bar{1})$ face, the computed (red scatter points) and fitted (curve) profiles of (b) electronic energies, (c) zero-point energies (ZPE), and the thermal correction to Gibbs free energies (G_corr) along the adsorption path at (d) 1200 K and (e) 1800 K.

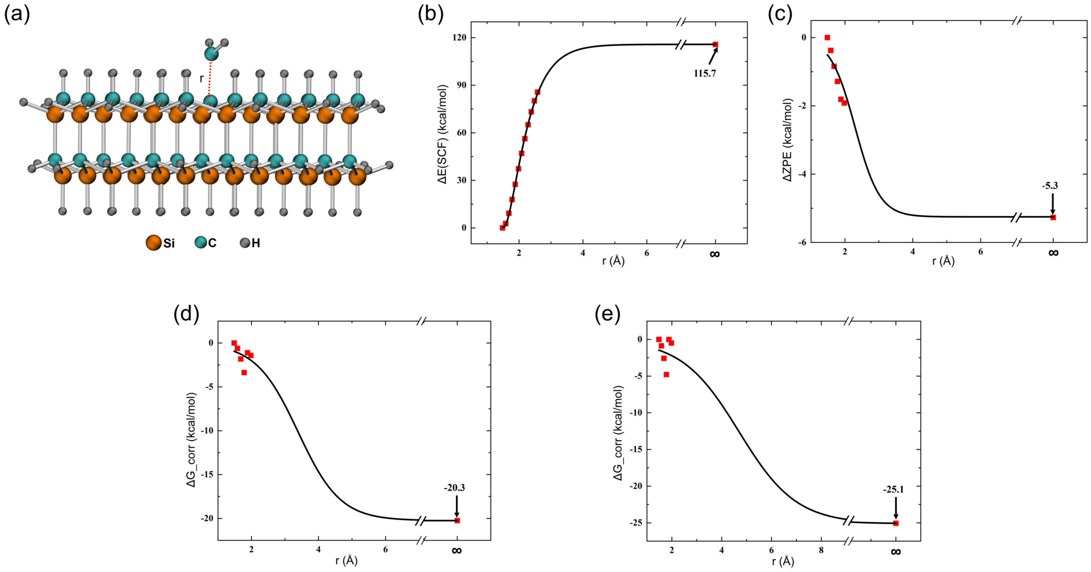

Figure S11. (a) Schematic illustration of the adsorption process of CH_2 on $(000\bar{1})$ face, the computed (red scatter points) and fitted (curve) profiles of (b) electronic energies, (c) zero-point energies (ZPE), and the thermal correction to Gibbs free energies (G_corr) along the adsorption path at (d) 1200 K and (e) 1800 K.

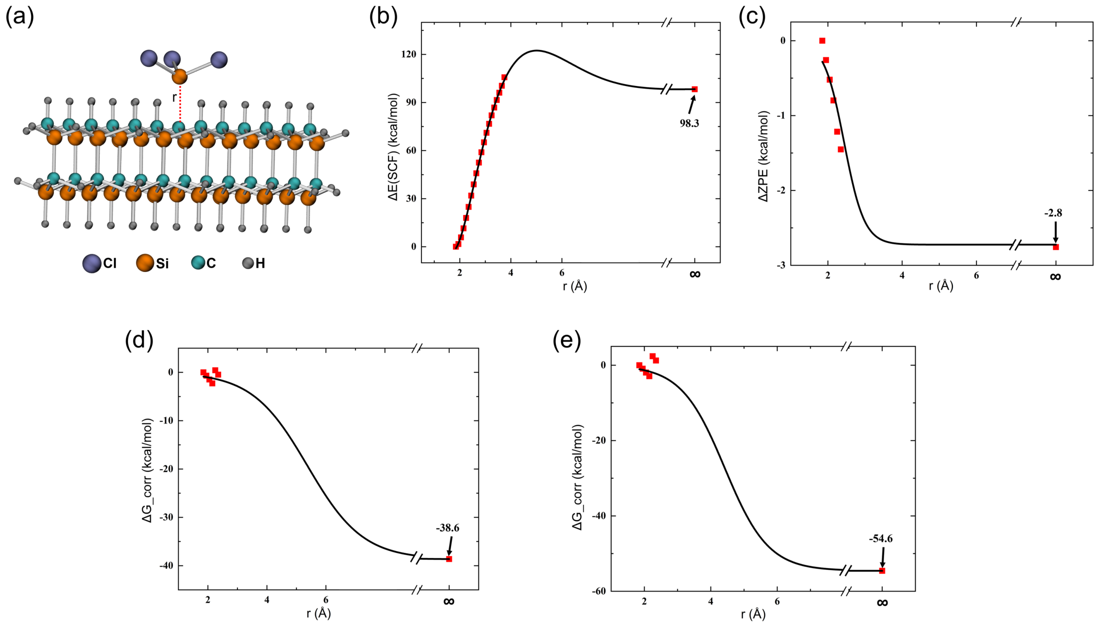

Figure S12. (a) Schematic illustration of the adsorption process of SiCl$_3$ on $(000\bar{1})$ face, the computed (red scatter points) and fitted (curve) profiles of (b) electronic energies, (c) zero-point energies (ZPE), and the thermal correction to Gibbs free energies (G_corr) along the adsorption path at (d) 1200 K and (e) 1800 K.

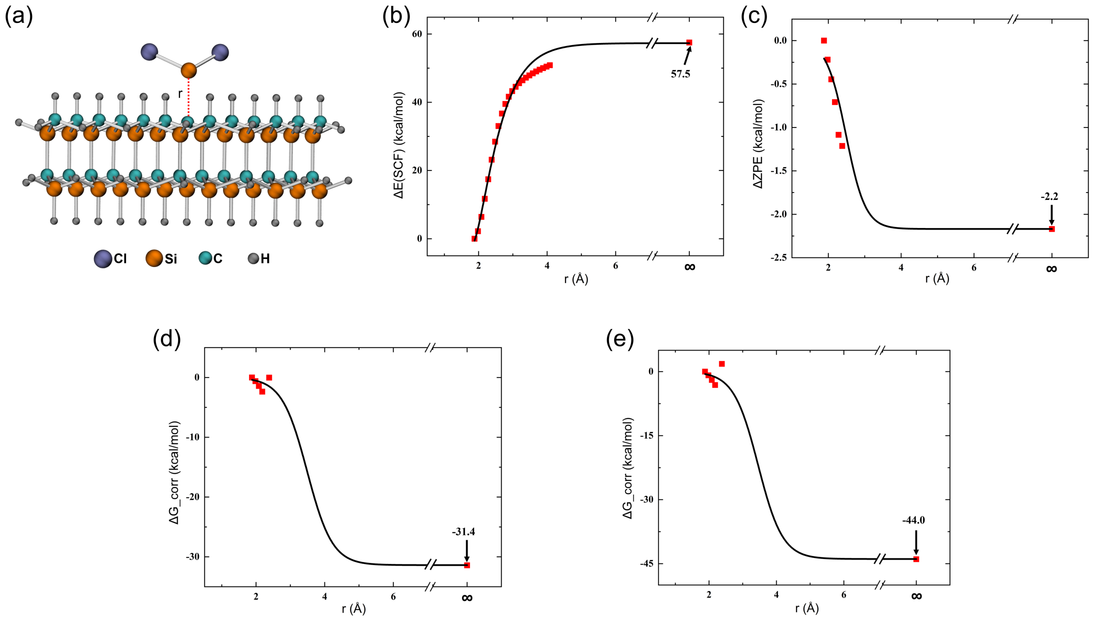

Figure S13. (a) Schematic illustration of the adsorption process of SiCl$_2$ on $(000\bar{1})$ face, the computed (red scatter points) and fitted (curve) profiles of (b) electronic energies, (c) zero-point energies (ZPE), and the thermal correction to Gibbs free energies (G_corr) along the adsorption path at (d) 1200 K and (e) 1800 K.

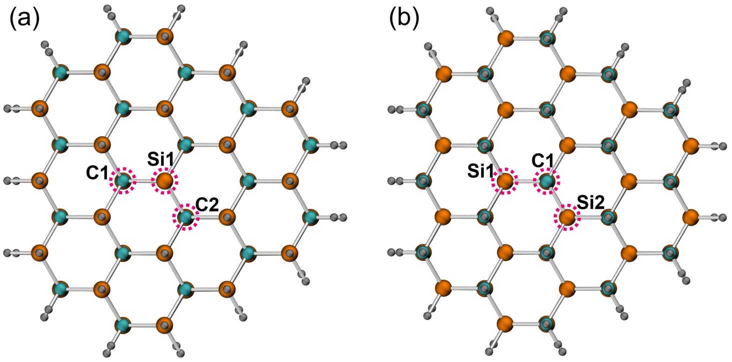

Figure S14. Depiction of the position of the atoms of the substrates: (a) (0001) face cluster, (b) (000$\bar{1}$) face cluster.

Table S2 The interatomic distances (depicted as l) and bond angles (depicted as ∠) of the optimized structures of different surface species as depicted in Figure S14(a).

	O_{Si}(ads)	Cl_{Si}(ads)	H_{Si}(ads)	CH_3(ads)	CH_2(ads)	$SiCl_2CH_3$(ads)
l_C1Si1	1.891	1.871	1.885	1.893	1.890	1.894
∠C1Si1C2	110.037	111.200	109.980	109.124	109.798	108.916
	$SiCl_2CH_2$(ads)	$SiCl_3$(ads)	$SiCl_2$(ads)	C_2H_4(ads)	CH_2Cl(ads)	C_2H_5(ads)
l_ C1Si1	1.891	1.888	1.889	1.895	1.885	1.897
∠C1Si1C2	109.236	109.607	110.069	108.904	109.670	108.686
	$SiHCl_2$(ads)					
l_ C1Si1	1.884					
∠C1Si1C2	109.615					

Table S3 The interatomic distances (depicted as l) and bond angles (depicted as ∠) of the optimized structures of different surface species as depicted in Figure S14(b).

	O_C(ads)	Cl_C(ads)	H_C(ads)	$SiCl_2CH_3$(ads)	$SiCl_2CH_2$(ads)	$SiCl_3$(ads)
l_ C1Si1	1.853	1.898	1.883	1.933	1.930	1.939
∠Si1C1Si2	114.586	111.287	110.623	107.543	107.541	107.534
	$SiCl_2$(ads)	CH_3(ads)	CH_2(ads)	C_2H_4(ads)	CH_2Cl(ads)	C_2H_5(ads)
l_ C1Si1	1.931	1.894	1.914	1.898	1.908	1.900
∠Si1C1Si2	108.276	109.157	108.827	108.897	108.830	108.302
	$SiHCl_2$(ads)					
l_ C1Si1	1.915					
∠Si1C1Si2	108.404					

References

[1] H. Ryu, J. Park, H.K. Kim, J.Y. Park, S.-T. Kim, M.-H. Baik, Pitfalls in computational modeling of chemical reactions and how To avoid them, Organometallics, 37 (2018) 3228-3239.

[2] P.M. Morse, Diatomic molecules according to the wave mechanics. II. vibrational levels, Physical Review, 34 (1929) 57-64.